Publishing House
AKAPIT

COMPUTER METHODS IN MATERIALS SCIENCE

Informatyka w Technologii Materiałów

Vol. 10, 2010, No. 1

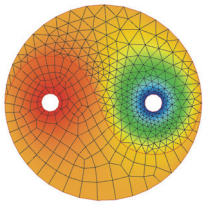

THE MODEL OF THE TEMPERATURE FIELD AND FLUID FLOW IN ELEMENTS HEATED BY MOVING HEAT SOURCES

WIESŁAWA PIEKARSKA*, MARCIN KUBIAK, ZBIGNIEW SATERNUS

Institute of Mechanics and Machine Design,
Czestochowa University of Technology
Dąbrowskiego 69, 42-200 Częstochowa
**Corresponding Author: piekarska@imipkm.pcz.czest.pl*

Abstract

This paper presents numerical analysis of thermal phenomena in hybrid laser – arc welding. The temperature field was obtained by solving the heat transfer equation with convection term. The fluid flow in the melted zone was determined by the solution of the Navier – Stokes equation taking into account the natural convection and flow through porous medium in the mushy zone. On the basis of elaborated models, the results of computer simulations were presented considering temperature and velocity distribution with marked fusion zone and the heat-affected zone.

Key words: Hybrid welding, thermal phenomena, numerical modelling

1. INTRODUCTION

Hybrid laser-arc welding is a modern welding technique that combines the common well known arc welding method, which is characterized by the high level of quality at a low weldment cost, with a laser welding technique, which allows for achievement of a deep material penetration at high welding speed (Bagger et al., 2005; Kusiński, 2000; Pilarczyk et al., 2007; Wouters, 2005). There are few works focused on understanding the transport phenomena occurring in this process, such as heat transfer in the heated material and fluid flow in the melted zone, which has a major influence on optimization of the hybrid welding technique. Experimental research of the hybrid laser-arc welding process is expensive, which is why the transport phenomena are analyzed theoretically by the mathematical and numerical modelling of the temperature field and the fluid flow in the welding pool.

In this study the mathematical and numerical model of thermal phenomena in hybrid laser-arc welding process is presented. The temperature field was obtained by the solution of the transient heat transfer equation with inner heat sources in Eulerian coordinates. The finite element method (Zienkiewicz & Taylor, 2000) was used to receive numerical solution to the transient heat transfer equation. Latent heat of fusion and latent heat of phase transformations were taken into account in the numerical algorithm. The velocity field was obtained by solution of the Navier-Stokes equation with the natural convection of liquid material in the melted zone as well as the fluid flow through porous medium in the mushy zone taken into consideration. The Chorin's projection method and the finite volume method (Zhou & Tsai, 2008) were established for numerical solution of the Navier-Stokes equation. Adequate models of volumetric heat source distribution were assumed for the electric arc (Gery

ISSN 1641-8581

et al., 2005) and the laser beam (Ranatowski, 2002) in the numerical computations. The computer simulations of the temperature field and melted material velocity field were carried out in this study. Modelled thermal phenomena are presented in a scheme of the considered system (figure 1).

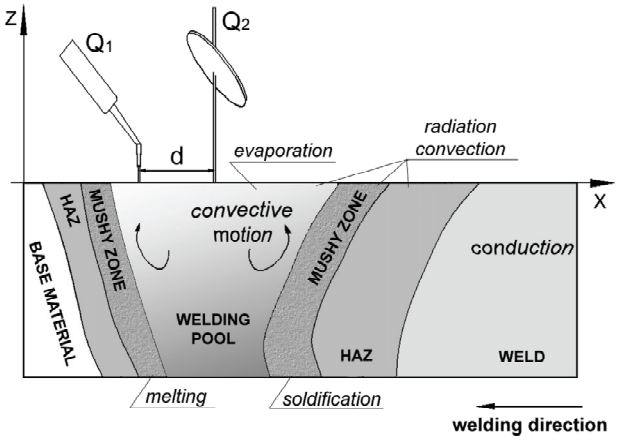

Fig. 1. *Scheme of the considered system*

2. MATHEMATICAL MODEL

The velocity field of the melted material in welding pool was obtained by the solution of the Navier-Stokes equation for laminar flow of incompressible viscous fluid with convective motions (Boussinesq's model) and the fluid flow through porous medium based on Darcy's model (DebRoy et al., 1995; Zhou & Tsai, 2008), described by the following formula:

$$\frac{\partial(\rho\mathbf{v})}{\partial t}+\nabla(\rho\mathbf{v}\mathbf{v})=-\nabla p+\mu\nabla^2\mathbf{v}+$$

$$\rho\mathbf{g}\beta_T\left(T-T_{ref}\right)-\frac{\mu}{K}\mathbf{v} \qquad (1)$$

where ρ is a density [kg/m^3], $\mathbf{g}$ is the acceleration of gravity vector [m/s^2], β_T is a volume expansion coefficient due to heating [1/K], T_{ref} is a reference temperature, μ is a dynamic viscosity [kg/ms] and K is a porous medium permeability.

The Navier–Stokes equation is completed by the boundary condition of Dirichlet's type: $\mathbf{v}=0$, implemented at the welding pool boundary and for the initial condition $t=0:\mathbf{v}=0$. Equation (1) must perform the continuity equation:

$$\nabla\cdot\mathbf{v}=0 \qquad (2)$$

The boundary of the melted zone is determined by temperature *Ts* (solidus). The Navier-Stokes equation is solved in the domain defined by the weld pool shape. The porous medium permeability is evaluated by (3) with linear approximation of solid phase in the mushy zone, described by the Carman–Kozeny relation:

$$K=K_0\frac{f_l^3}{(1-f_l)^2};\quad K_0=\frac{d^2}{180} \qquad (3)$$

where: $f_l=1-f_S$ is a porosity coefficient, f_s is a solid fraction in the mushy zone, d is average diameter of solid particle in the mushy zone [m], K_0 is basic permeability of porous medium.

The temperature field was obtained by solving the transient heat transfer equation with convection term, described as follows:

$$\nabla(\lambda\nabla T)=C_{ef}\left(\frac{\partial T}{\partial t}+\mathbf{v}\nabla T\right)-\widetilde{Q} \qquad (4)$$

where $\lambda=\lambda(T)$ is a thermal conductivity [W/mK], $C_{ef}=C_{ef}(T)$ is a heat capacity which includes latent heat of fusion and latent heat of phase transformations, $\widetilde{Q}=Q+Q_v^p$ is volumetric heat source [W/m^3], where Q is the heating source described as $Q=Q_1+Q_2$ and Q_v^p gives consideration to material evaporation heat in the keyhole, $\mathbf{v}=\mathbf{v}(x_\alpha,t)$ is a velocity vector [m/s], x_α is material point coordinates in Cartesian coordinate system.

Equation (4) is completed by the initial condition $t=0:T=T_0$ and the boundary conditions of Dirichlet, Neumann and Newton type, taking into account a heat loss due to convection, radiation and evaporation:

$$T\big|_\Gamma=\widetilde{T},\quad q=-\lambda\frac{\partial T}{\partial n}\bigg|_\Gamma=\widetilde{q} \qquad (5)$$

$$-\lambda\frac{\partial T}{\partial n}=-q_o^s+\alpha_k(T\big|_\Gamma-T_0)+$$

$$\varepsilon\sigma(T^4-T_0^4)+q_v^s \qquad (6)$$

where α is convective coefficient, assumed as α_k = 100 [W/m^{2}K] in computations, ε is radiation coefficient (ε = 0.5), and σ is Stefan-Boltzmann constant. Element q_o^s is the heat flux towards the top surface of the welded element (z = *0*) in the source activity field, while q_v^s represents heat loss due to material evaporation in area where $T\geq T_L$, Γ is a boundary of analysed domain.

Latent heat of fusion was introduced into the model assuming linear approximation of solid phase between the solidus and the liquidus temperatures (T_S and T_L). The simulation parameters were accepted as: T_S = 1750 and T_L = 1800 K, c_S = 650 and c_L = 840 J/kgK, ρ_S = 7800 and ρ_L = 6800 kg/m^3, H_L = 270×10^3 J/kg (latent heat of fusion). Latent heat of phase transformation in the solid state (austenite into ferrite, bainite and martensite) were assumed according to experimental data (Piekarska, 2007), that is: $H_{A\rightarrow}$ = 8·10^4, $H_{A\rightarrow P}$=9·10^4 and $H_{A\rightarrow B}$ = $H_{A\rightarrow M}$ = 11.5·10^4 J/kg.

Two different models of heat sources were applied to numerical computations. Goldak's model was used to describe the electric arc heat source power distribution:

$$q_1(x,y,z)=\frac{6\sqrt{3}f_1Q_k}{abc_1\pi\sqrt{\pi}}\exp(-3\frac{x^2}{a^2})\exp(-3\frac{y^2}{b^2})\exp(-3\frac{z^2}{c_1^2})$$
$$q_2(x,y,z)=\frac{6\sqrt{3}f_2Q_k}{abc_2\pi\sqrt{\pi}}\exp(-3\frac{x^2}{a^2})\exp(-3\frac{y^2}{b^2})\exp(-3\frac{z^2}{c_2^2}) \quad (7)$$

where a, b, c_1 and c_2 are set of axes defining front ellipsoid and rear ellipsoid, f_1 and f_2 ($f_1+f_2=2$) represents energy distribution at the front and the rear section of the heat source, thus resultant distribution of the source energy is the total sum described as $Q_1(x,y,z)=q_1(x,y,z)+q_2(x,y,z)$ and $Q_k=\eta IU$ is the power of electric arc [W], where I is current intensity [A], U is voltage [V] and η is efficiency of the arc.

Cylindrical-involution-normal model was used to describe the laser beam heat source power distribution:

$$Q_2(r,z)=\frac{kK_zQ_L}{\pi\left(1-e^{(K_zs)}\right)}e^{-\left(kr^2+K_zz\right)}\left(1-u\left(z-s\right)\right) \quad (8)$$

where Q_L is the power of laser beam [W], r_0 is the beam radius [m] and $r=\sqrt{x^2+y^2}$ is the current radius [m], $K_z=3/s$ is the power exponent of heat source [m^{-1}], $k=3/r_0^2$ is the coefficient of beam concentration [m^{-2}] and s is the laser beam penetration depth [m], $u\left(z-s\right)$ is the Heaviside's function, which assumes 1 outside the maximum laser beam penetration.

Exemplary power distribution of the heat source in geometrical set-up with leading arc source is presented in figure 2.

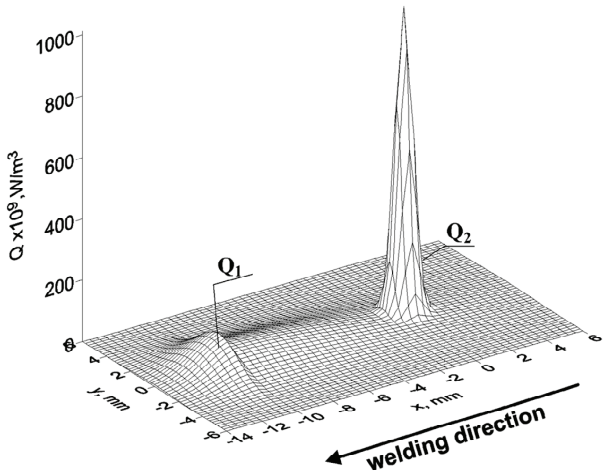

Fig. 2. Exemplary heat source power distribution

3. NUMERICAL MODEL

Equation (1) was solved by Chorin's projection with the finite volume method. In the first stage of projection, the Navier-Stokes equation is solved without momentum changes due to pressure forces, as follows:

$$\frac{\mathbf{v}^*-\mathbf{v}^n}{\Delta t}=-\nabla\left(\mathbf{vv}\right)^n+$$
$$\frac{1}{\rho^n}\left(\mu\nabla^2\mathbf{v}^n+\rho^n\mathbf{g}\beta_T\left(T-T_{ref}\right)-\frac{\mu}{K}\mathbf{v}^n\right) \quad (9)$$

where $\mathbf{v}^*$ is a temporary velocity obtained from changes in velocity $\mathbf{v}^n$ resulting from advection, viscosity and body force terms.

In the second stage, the projection of velocity $\mathbf{v}^*$ onto $\mathbf{v}^{n+1}$ is made according to the formula

$$\frac{\mathbf{v}^{n+1}-\mathbf{v}^*}{\Delta t}=-\frac{1}{\rho^n}\left(\nabla p^{n+1}\right) \quad (10)$$

The formula (10) with the continuity equation described in (2) is combined into one Poisson equation:

$$\nabla\left(\frac{1}{\rho^n}\left(\nabla p^{n+1}\right)\right)=\frac{1}{\Delta t}\nabla\mathbf{v}^* \quad (11)$$

The Poisson equation is used to find the pressure, at which the velocity at the new time step is divergence free.

Equation (4) was solved by the finite element method. The weak form of equation (4) is obtained by the weighed residuum criterion

$$\int_{\Omega} \varphi\left[\nabla(\lambda\nabla T)+\tilde{Q}\right]d\Omega = \int_{\Omega} \varphi C_{ef}\dot{T}d\Omega \quad (12)$$

where $\varphi = \varphi(\mathbf{x})$ is a weight function.

The Petrov–Galerkin formulation was used in equation (12) to ensure stability of the numerical algorithm. Because temperature in every node of FE mesh is time function $T_j = T_j(t)$, time integration of equation (12) must be carry out, leading to the following formula:

$$\sum_e \left(K_{ij}^e + V_{ij}^e\right)\int_t \vartheta(t)T_j(t)dt + \sum_e M_{ij}^e \int_t \vartheta(t)\frac{\partial T_j(t)}{\partial t}dt = \\ = \sum_e S_{ij}^e \int_t \vartheta(t)Q_j^e(t)dt - \sum_{e^\Gamma} S_{ij}^\Gamma \int_t \vartheta(t)\tilde{q}_j^e(t)dt \quad (13)$$

where $\vartheta = \vartheta(t)$ is time weight function, K_{ij}^e is the local conductivity matrix, V_{ij}^e is convection matrix, M_{ij}^e is heat capacity matrix, S_{ij}^e is matrix of coefficients, $Q_j^e(t)$ is vector of inner heat sources, $\tilde{q}_j^e(t)$ is vector of boundary fluxes.

The final form of solution to the problem, after time integration, is expressed in the form:

$$\left(\beta K_{ij} + M_{ij}\right)T_j^{s+1} = \left[M_{ij} - (1-\beta)K_{ij}\right]T_j^s + \\ \beta Q_i^{s+1} + (1-\beta)Q_i^s - \beta q_i^{*s+1} - (1-\beta)q_i^{*s} \quad (13)$$

where β is time integration coefficient.

The solution algorithm presented in figure 3 consists of two modules responsible for numerical solution of the transient heat transfer equation in FEM (14) and Navier-Stokes equation (9) in Chorin's projection and FVM. Analyzed domain was approximated by staggered grid, where velocity is calculated at the edges of bilinear finite elements and temperature is calculated at the element nodes. Moreover, the pressure obtained by numerical solution of equation (11) is calculated in the center of each element.

4. EXAMPLES OF NUMERICAL COMPUTATIONS

The parameters of heat sources were assumed as: Q_1 = 3 kW, a = 4 mm, b = 2 mm, c_1 = 4 mm, c_2 = 16 mm, f_1 = 0.6, f_2 = 1.4 for the electric arc and Q_2 = 1 kW, r_0 = 1 mm for the laser beam, and the welding speed was assumed as v = 0.7 m/min. The laser-to-arc distance was equal to d = 5 mm.

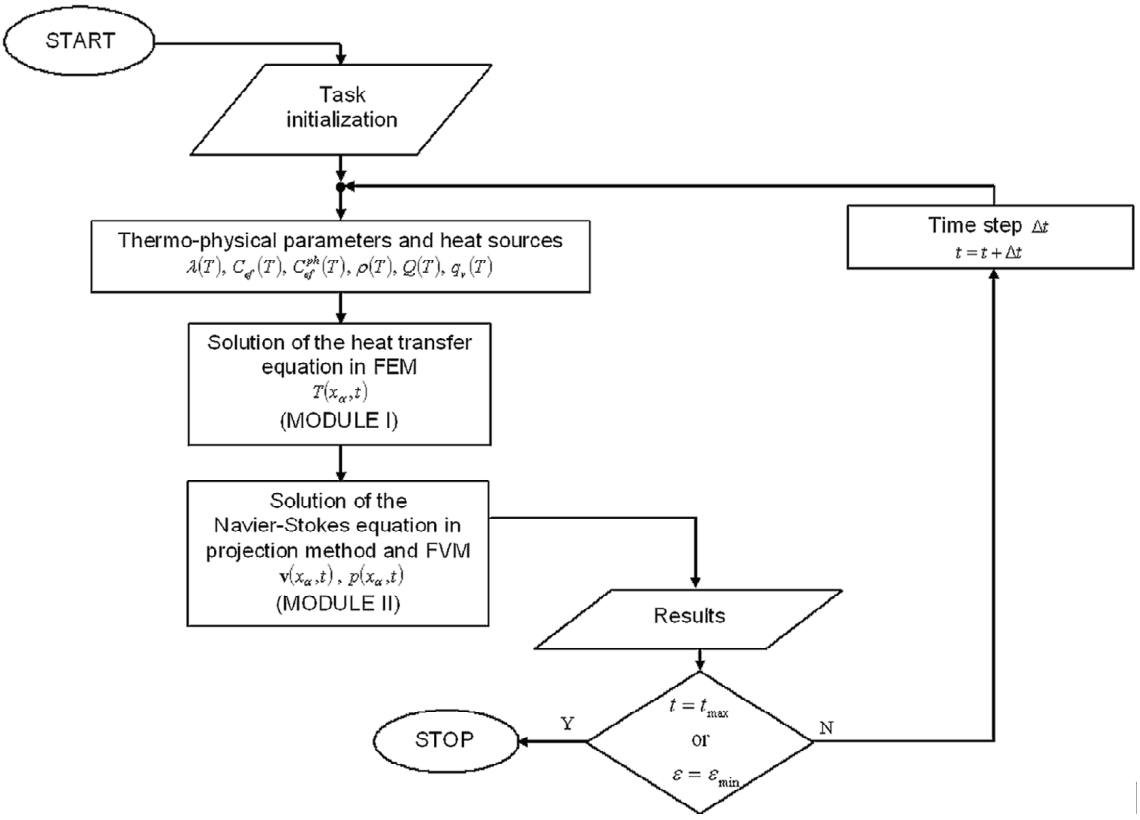

Fig. 3. *Solution algorithm*

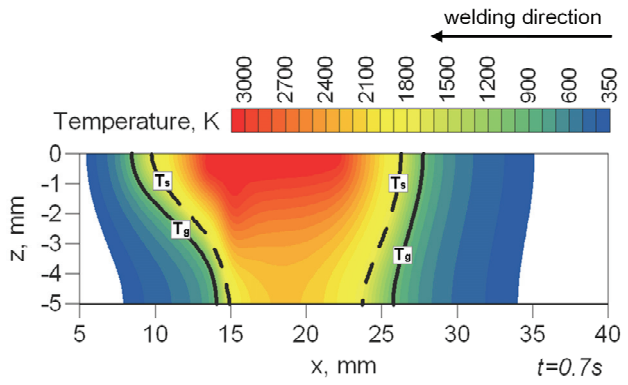

Fig. 4. *Temperature distribution in longitudinal section of the weld at time t = 0.7s*

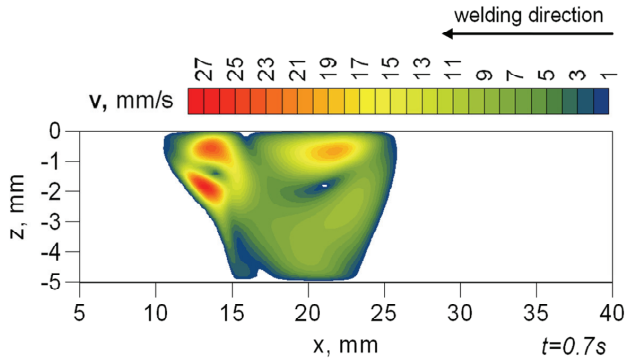

Fig. 5. *Velocity field in melted zone of the weld at time t = 0.7s*

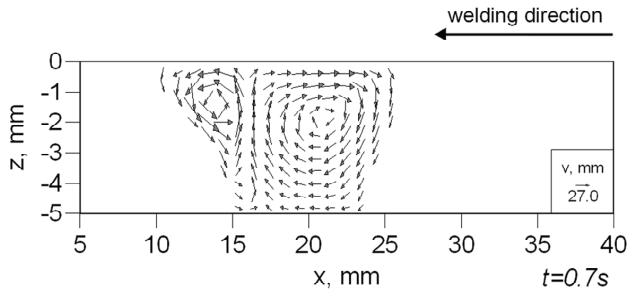

Fig. 6. *Velocity vectors in melted zone of the weld at time t = 0.7s*

Figure 4 presents the temperature distribution with marked solidus temperature (T_s) which determines the melted zone and temperature T_g = 1000K which in turn determines the starting point for the austenite formed during heating (Ac_1). Figures 5 and 6 illustrate the velocity field in the melted zone of the weld at time t = 0.7s

5. CONCLUSIONS

The mathematical and numerical models presented in this study allow analyzing the transport phenomena of heat transfer and the fluid flow in the melted zone present in the hybrid laser-arc welding process. The influence of convective motion in the welding pool on the weld shape and on the heat affected zone can be observed (figures 4÷6). The presented results of analysis into the temperature field and the velocity field allow the kinetics of phase transformations in solid state to be defined and the composition of material structure in the hybrid laser-arc welded joint to be predicted.

REFERENCES

Bagger, C., Olsen, F.O., 2005, Review of laser hybrid welding, *Journal of Laser Applications*, 17, 1.

Gery, D., Long, H., Maropoulos, P., 2005, Effects of welding speed, energy input and heat source distribution on temperature variations in butt joint welding, *Journal of Materials Processing Technology*, 167, 393-401.

DebRoy, T., Davis, S.A., 1995, Physical processes in fusion welding, *Reviews of Modern Physics*, 67, 85-112.

Kusiński, J., 2000, *Lasery i ich zastosowanie w inżynierii materiałowej*, wyd. Akapit, Kraków.

Ranatowski, E., 2002, Uwagi o modelowaniu procesów cieplnych przy użyciu skoncentrowanych źródeł energii, *Przegląd Spawalnictwa*, 8-10, 152-155.

Wouters, M., 2005, *Hybrid laser-MIG welding: An investigation of geometrical considerations*, Lulea, Sweden.

Pilarczyk, J., Banasik, M., Dworak, J., Stano, S., 2007, Spawanie hybrydowe z wykorzystaniem wiązki laserowej i łuku elektrycznego, *Przegląd Spawalnictwa*, 10, 44-48.

Piekarska, W., 2007, *Analiza numeryczna zjawisk termomechanicznych procesu spawania laserowego. Pole temperatury, przemiany fazowe i naprężenia*, Praca habilitacyjna 135, Wydawnictwo Politechniki Częstochowskiej, Częstochowa.

Zienkiewicz, O.C., Taylor, R.L., 2000, *The finite element method, Butterworth-Heinemann, Fifth edition*, 1, 2, 3, New York.

Zhou, J., Tsai, H.L., 2008, Modeling of transport phenomena In hybryd laser – MIG keyhole welding, *International Journal of Heat and Mass Transfer*, 51, 4353-4366.

MODEL POLA TEMPERATURY I RUCH CIECZY W ELEMENTACH NAGRZEWANYCH RUCHOMYMI ŹRÓDŁAMI CIEPŁA

Streszczenie

Praca dotyczy numerycznej analizy zjawisk cieplnych w procesie spawania hybrydowego laser – łuk elektryczny. Pole temperatury wyznaczono z rozwiązania równania nieustalonego przewodzenia ciepła z członem konwekcyjnym. Ruch cieczy w obszarze przetopienia wyznaczono z rozwiązania równania Naviera – Stokesa z uwzględnieniem konwekcji swobodnej cieczy oraz przepływu cieczy przez medium porowate w obszarze dwufazowym. Na podstawie opracowanych modeli przedstawiono wyniki symulacji komputerowej obejmujące pole temperatury oraz pole prędkości cieczy z zaznaczoną strefą przetopienia i strefą wpływu ciepła.

Received: February 12, 2010
Received in a revised form: June 7, 2010
Accepted: June 9, 2010